Available online at www.sciencedirect.com
ScienceDirect
Catalysis Today 131 (2008) 437–443
CATALYSIS TODAY
www.elsevier.com/locate/cattod

Synthesis of Ti-containing SBA-15 materials and studies on their photocatalytic decomposition of orange II

Won Young Jung [a], Seung Hee Baek [a], Jin Sup Yang [a], Kwon-Taek Lim [b], Man Sig Lee [c], Gun-Dae Lee [a], Seong Soo Park [a], Seong-Soo Hong [a,*]

[a] *Division of Applied Chemical Engineering, Pukyong National University, 100 Yongdang-dong, Nam-ku, 608-739 Busan, South Korea*
[b] *Information Engineering, Pukyong National University, 100 Yongdang-dong, Nam-ku, 608-739 Busan, South Korea*
[c] *Busan R&D Center, Korea Institute of Industrial Technology*

Available online 26 November 2007

Abstract

Titanium substituted SBA-15 mesoporous materials have been successfully prepared by conventional hydrothermal method and they were also used as support on TiO_2 loaded SBA-15 photocatalysts. The synthesized materials were characterized by XRD, UV–vis DRS, FT-IR, BET and TEM. We also examined the activity of these materials as photocatalysts for the decomposition of orange II. The incorporation of titanium into framework of SBA-15 makes the pore diameter and pore volume to decrease and slightly decreases the surface area compared to SBA-15. In addition, the pore size distribution becomes broaden with an increase of titanium amount in the SBA-15 framework. For Ti-SBA-15 and TiO_2 loaded Ti-SBA-15 photocatalysts, the IR absorption at ~960 cm^{-1} commonly accepted the characteristic vibration of Ti–O–Si bond. From the TEM images, the regular silica morphology is maintained in the case of Ti-SBA-15(Si/Ti = 50) but the Ti-SBA-15 sample having Si/Ti ratio = 10 partially destroys the hexagonal highly ordered structure and the mesopore structure is disappeared by the clogging of mesopore channels by the titanium dioxides particles for the 50 wt.% TiO_2/Ti-SBA-15 samples. The photocatalytic activity increases with an increase of Ti content (decrease of Si/Ti ratio) and with an increase of TiO_2 loading content.

Keywords: Ti substituted SBA-15; TiO_2 loaded Ti-SBA-15; Photocatalytic decomposition of orange II

1. Introduction

Heterogeneous photocatalysis, a semiconductor mediated catalytic process, is shown to be a promising technology to degrade a wide range of organic pollutants [1,2]. Among various metal oxide semiconductors, titania, especially anatase phase, has been proven to be one of the most efficient photocatalysts due to its chemical stability, relatively low price, non-toxicity and optical and electronic properties. To maximize TiO_2 photocatalytic activity, particles should be small enough to offer a high specific surface area. Unfortunately, for applications in aqueous phase such as a small particle size means high filtration costs to remove the catalyst once the reaction is finished. These problems have motivated the development of supported photocatalysts in which TiO_2 has been immobilized on diverse materials [3].

Incorporation of transition-metal ions into the frameworks of the molecular sieves is a general method for introducing catalytic sites into mesoporous material. Especially, the introduction of Ti-containing mesoporous materials has added a new dimension to the application of mesoporous materials in oxidation catalysis [4]. Recently, it has been reported that incorporation of photoactive elements into MCM-41 [5] framework gives it unique photocatalytic activity. However, poor hydrothermal stability of MCM-41 has so far restricted its application potential from a commercial point of view. These efforts have resulted in a successful synthesis of hydrothermally stable SBA-15 silica molecular sieve with uniform hexagonal channels ranging from 50 to 300 Å [6]. Newalkar et al. [7] have recently obtained Ti-containing SBA-15 materials using a microwave assisted method. However, the challenge to prepare metal substituted SBA-15 materials directly via the usual hydrothermal method remains. Chen et al. [8] synthesized Ti-substituted SBA-15 under conventional hydrothermal conditions using titanium tetrachloride and tetraethyl orthosilicates

* Corresponding author.
E-mail address: sshong@pknu.ac.kr (S.-S. Hong).

0920-5861/$ – see front matter © 2007 Elsevier B.V. All rights reserved.
doi:10.1016/j.cattod.2007.10.072

as the titanium and silica sources. To obtain high-quality Ti-SBA-15 materials, the maximum ratio of Ti/Si in the initial gel was observed to be above 0.015. Owing to its structural characteristics, Ti-substituted SBA-15 could serve as a versatile selective oxidation catalyst. However, the effort to use Ti-substituted SBA-15 as a photocatalytic catalyst has not reported. In addition, it has been claimed that photocatalytic activity of TiO_2 increased when it was loaded on zeolite or mesoporous silica support [5,9,10].

In this study, Ti-containing SBA-15 samples were prepared by hydrothermal method and then TiO_2 was loaded on these materials. The physical properties of prepared Ti-containing SBA-15 and TiO_2 loaded Ti-SBA-15 samples were investigated and we also examined the activity of them as photocatalysts for the decomposition of orange II.

2. Experimental

2.1. Preparation of catalysts

Ti-substituted SBA-15 materials with varying Si/Ti ratio in the range of 50–10 were synthesized by hydrothermal method using tetraethyl orthosilicate (TEOS) and titanium tetraisopropoxide (TTIP) as the sources of Si and Ti, respectively. 4.06 g of Pluronic P123 triblock copolymer surfactant ($EO_{20}PO_{70}EO_{20}$, $M_{av} = 5800$) and 0.68 g of PEG (polyethyleneglycol) were dissolved in 160 mL of distilled water and 10 mL of 2 M HCl was added by drop wise to the solution as a catalyst. Under stirring, 22.78 mL of 0.1 M TEOS solution was added and the mixture was stirred continuously for 6 h to make the solution homogeneous. Then, the ethanol solution mixed a calculated amount of TTIP was added under vigorous stirring at 35–40 °C and stirring was continued for 24 h. The resultant mixture was then aged in the autoclave at 100 °C for 48 h. The crystallized product was filtered, washed with distilled water, dried at ambient temperature for 24 h, and finally calcined 500 °C for 3 h. In addition, TiO_2 loaded Ti-SBA-15 photocatalysts were prepared by impregnating on Ti-SBA-15 using ethanol solution of TTIP with a drop wise water and the range of TiO_2 loading was 10–50 wt.%.

2.2. Characterization of catalysts

The major phase of the obtained particles was analyzed by X-ray diffraction (Rigaku D/MAXIIC) using Cu-Kα radiation.

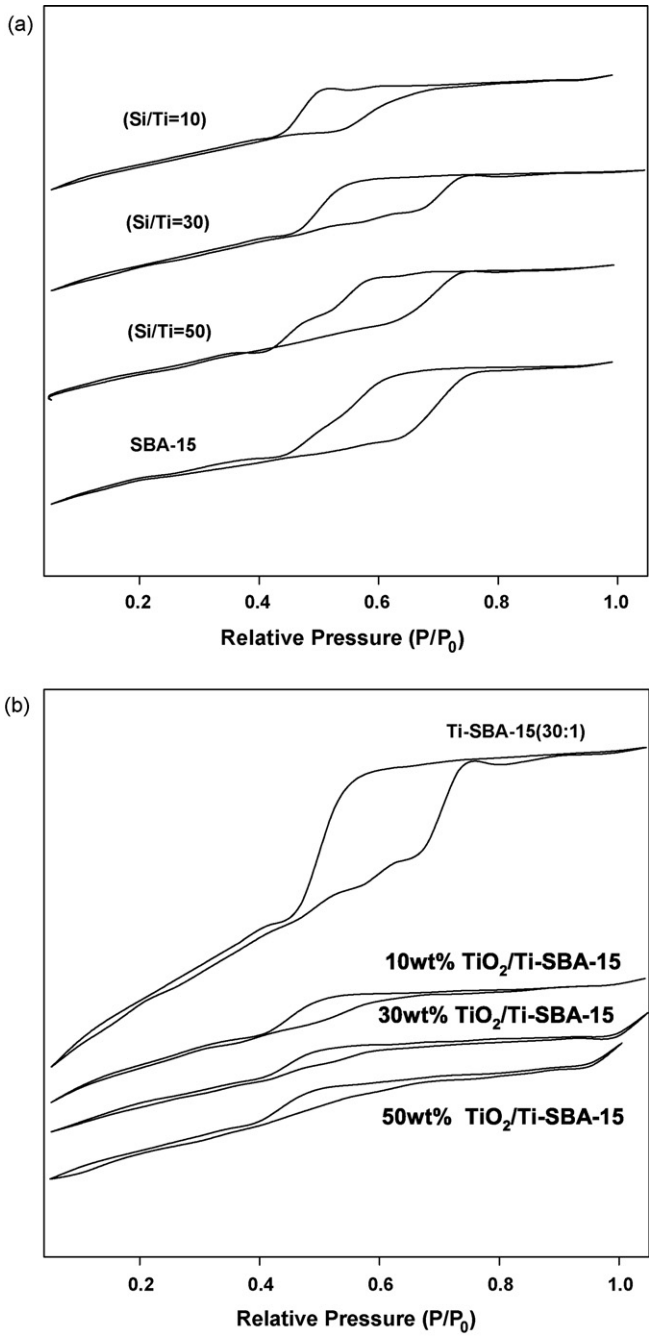

Fig. 1. N_2 adsorption/desorption isotherm of various Ti-SBA-15 (a) and TiO_2/Ti-SBA-15 materials (b).

Table 1
Textural properties of Ti-SBA-15 and TiO_2 loaded Ti-SBA-15 materials and their photocatalytic activity on the decomposition of orange II

Materials	Surface area (m^2/g)	Micropore volume ($\times 10^{-8}$ m^3/g)	Pore diameter[a] (nm)	Catalytic activity[b] k' (min^{-1}) $\times 10^{-3}$
SBA-15	896	9.3	4.2	5.9
Ti-SBA-15 (Si/Ti = 50)	892	8.9	4.0	8.5
Ti-SBA-15 (Si/Ti = 30)	888	8.8	3.8	12.3
Ti-SBA-15 (Si/Ti = 10)	885	7.8	3.5	17.2
10 wt.% TiO_2/Ti-SBA-15	498	3.6	3.4	13.4
30 wt.% TiO_2/Ti-SBA-15	440	3.5	3.3	17.5
50 wt.% TiO_2/Ti-SBA-15	385	3.5	3.2	20.4

[a] BJH adsorption average pore diameter.
[b] Apparent first-order constants (k') of orange II.

The chemical structure of the prepared particles was examined using the Fourier transform infrared spectrophotometer (FTIR, Bruker, IFS-88) in the 400–1500 cm^{-1} frequency range. The BET surface area of the prepared particles was determined by nitrogen physisorption data at 77 K using a Micromeritics ASAP 2400 and pore volume and pore size distribution were determined by the BJH (Barrett–Joyner–Halenda) method. UV–vis diffuse reflectance spectroscopy (DRS) was performed on Varian Cary 100 with PTFE (polytetrafluoroethylene) as standard. The pore morphology of the mesoporous materials and the titania particles supported on SBA-15 were observed on a Transmission electron microscope (TEM, JEOL, JEM-2020) of 200 kV accelerating voltage.

2.3. Photocatalytic activity test

A biannular quartz glass reactor with a lamp immersed in the inner part of the reactor was used for all the photocatalytic experiments. The batch reactor was filled with 450 ml of an aqueous dispersion in which the concentration of titania and of orange II were 1.0 g/L and 100 mg/L, respectively and magnetically stirred to maintain uniformity both concentration and temperature. A 500 W high-pressure mercury lamp (Kumkang Co.) was used. The circulation of water in the quartz glass tube between the reactor and the lamp allowed the lamp to stay cool and to warm the reactor to the desired temperature. Nitrogen was used as a carrier gas and pure oxygen was used as an oxidant. The samples were immediately centrifuged and the quantitative determination of orange II was performed by a UV–vis spectrophotometer (Shimazu UV-240).

3. Results and discussion

Table 1 shows the textural properties of the siliceous titanium substituted SBA-15 and TiO_2 loaded on Ti-SBA-15 samples. It is clear that the incorporation of titanium into framework of SBA-15 makes the pore diameter and pore volume to decrease, due to the fact that the diameter of a titanium atom is larger than that of a silicon atom, but slightly decreases the surface area compared to SBA-15. However, TiO_2 loaded on the silica matrix drastically decreases the surface area of the support as expected for TiO_2 incorporation. It is also

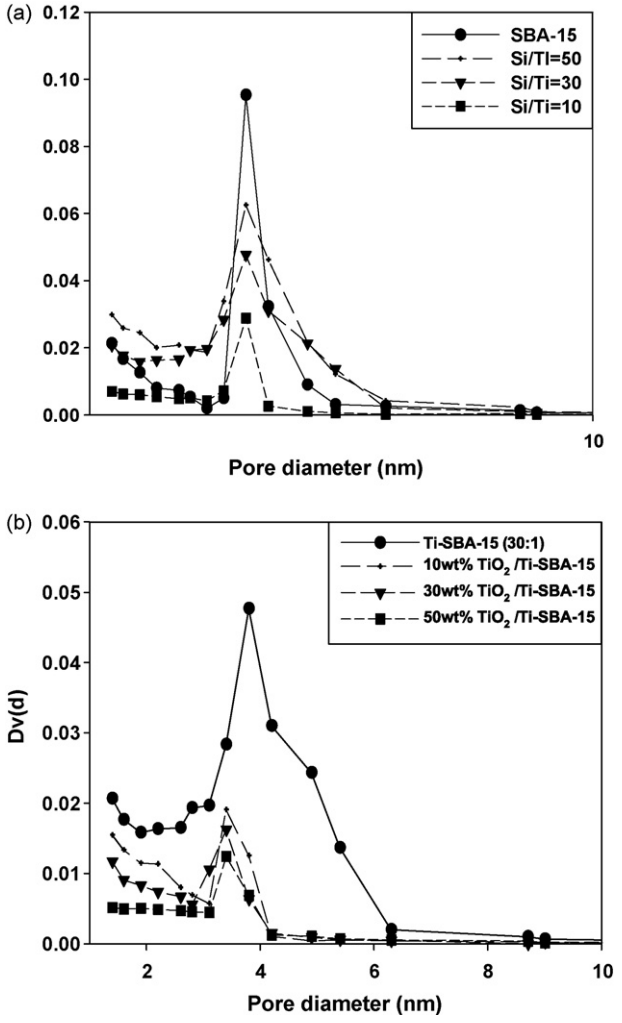

Fig. 2. Pore size distribution of various Ti-SBA-15 (a) and TiO_2/Ti-SBA-15 materials (b).

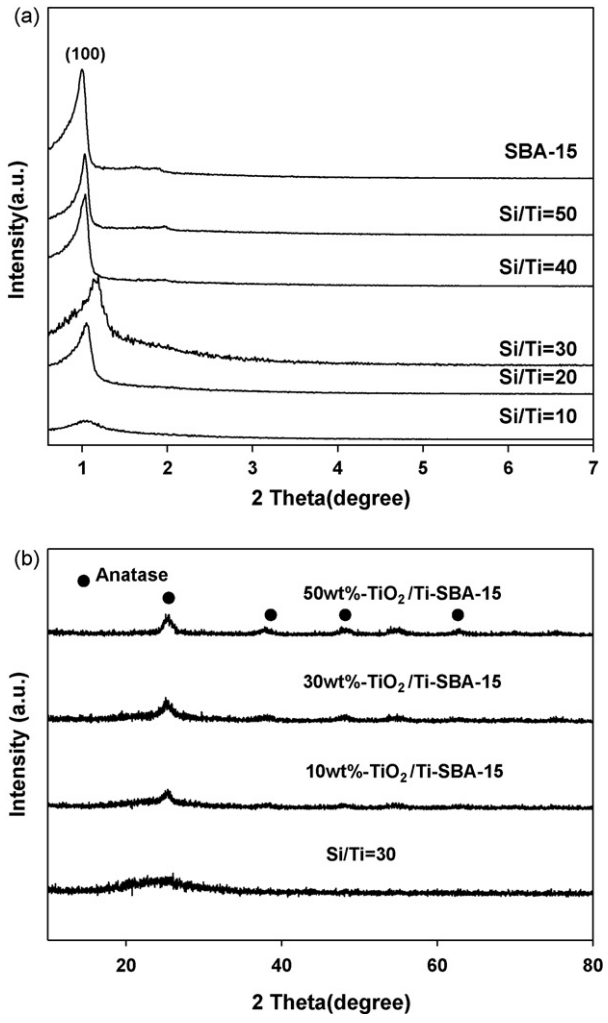

Fig. 3. X-ray diffraction patterns various Ti-SBA-15 (a) and TiO_2/Ti-SBA-15 materials (b).

observed that a rapid decrease in their pore volume values, when TiO_2 is loaded on Ti-SBA-15 samples. This pore volume reduction indicates that most of the semiconductor particles loading take place within the ordered channels of the support. This result can be confirmed by the TEM micrograph of 50 wt% loaded TiO_2 on Ti-SBA-15 (Fig. 6 (d)) which the highly ordered mesopore structure is disappeared by the clogging of mesopore channels by the titanium dioxides particles.

Fig. 1 shows the adsorption-desorption isotherms of Ti-SBA-15 and TiO_2/Ti-SBA-15 materials. As it can be observed, all materials exhibit the type IV nitrogen isotherm with desorption hysteresis loops types H1 in the case of the siliceous SBA-15 and Ti-SBA-15 materials, indicative of their mesoporosity. It is well known that the position of inflection point is clearly related to a diameter in the mesopore range and the sharpness of these slopes indicates the uniformity of the mesopore size distribution [11]. As shown in Fig. 1, the inflection points are similar but the sharpness of the steeps is decreased as the amount of substituted titania increases. This result indicates that the substitution of titanium atom into the SBA-15 makes broaden the mesopore size distribution. This result can be verified by the pore size distribution curve (Fig. 2(a)) which the pore size distribution becomes broaden with an increase of titanium amount in the SBA-15 framework.

TiO_2 loaded on Ti-SBA-15 material shows type IV nitrogen isotherm but they exhibits desorption hysteresis loops types H5. With an increase of titanium dioxide amount on Ti-SBA-15, the hysteresis loop becomes to be narrow. Therefore, it can be explained that the mesostructure is maintained but the pore size and pore volume is decreased due to the clogging of mesopore channels by the titanium dioxide particles.

Fig. 2 shows the pore size distribution of Ti-SBA-15 and TiO_2/Ti-SBA-15 materials. With an increase of titanium content (decrease of Si/Ti ratio), the pore size distribution becomes broaden due to the fact that the diameter of a titanium atom is larger than that of a silicon atom. This result indicates that the introduction of titanium into SBA-15 framework decreases the uniformity of the mesopore size distribution. For TiO_2 loaded Ti-SBA-15 samples, the pore diameter decreases and the peak intensities sharply decrease with an increase of titanium dioxide loading ratio. This may be attributed to the clogging of mesopore channels by the titanium dioxides particles.

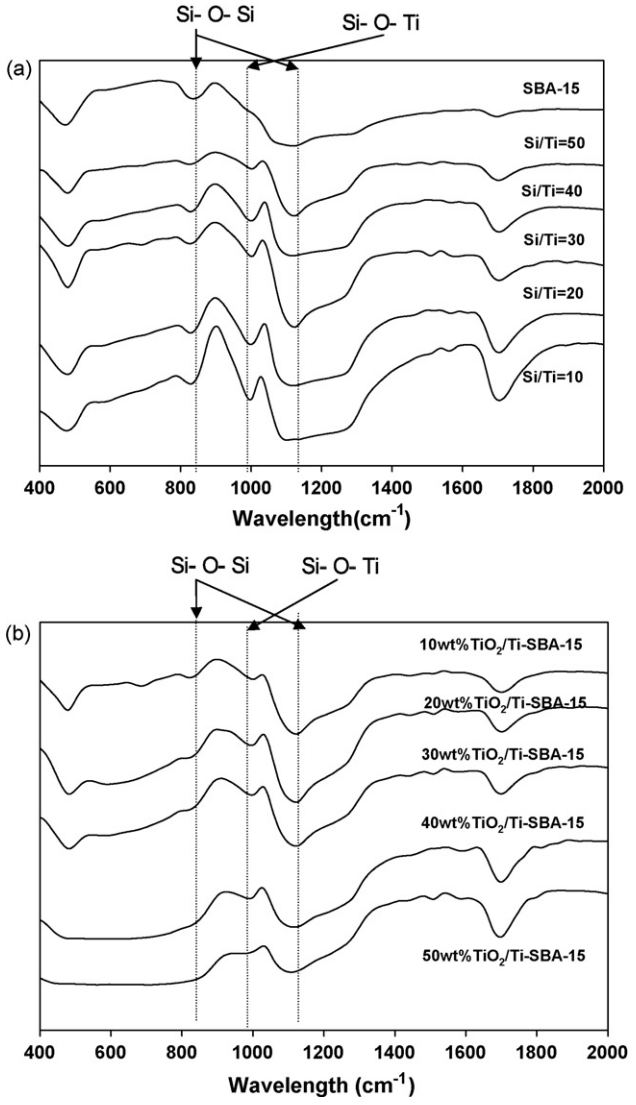

Fig. 4. FT-IR spectra of various Ti-SBA-15 (a) and TiO_2/Ti-SBA-15 materials (b).

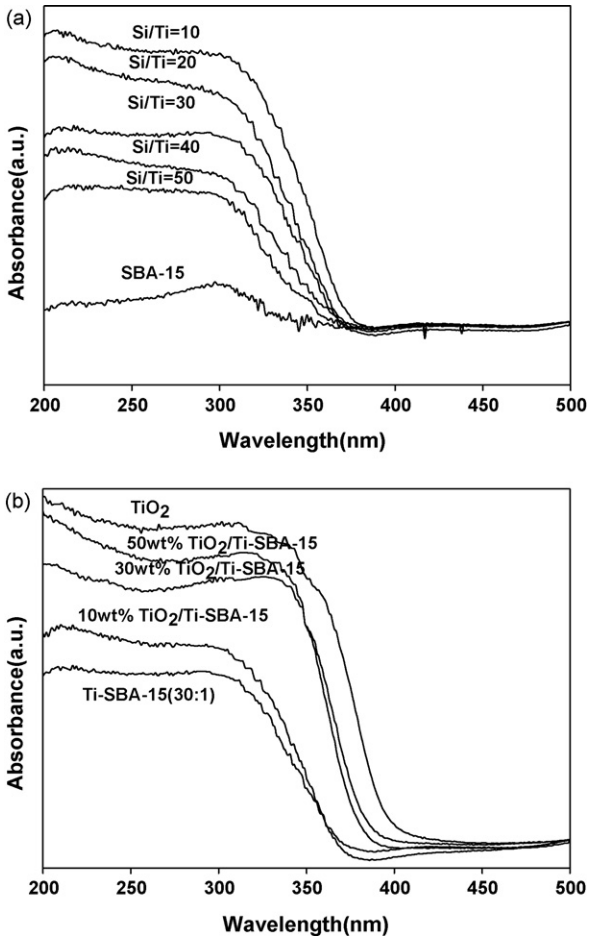

Fig. 5. UV-vis diffuse reflectance of various Ti-SBA-15 (a) and TiO_2/Ti-SBA-15 materials (b).

Fig. 3 shows XRD patterns of Ti-SBA-15 and TiO_2/Ti-SBA-15 materials. Calcined siliceous SBA-15 and Ti-SBA-15 samples with varying titanium loading displayed well-resolved pattern with a sharp peak at about 1.0° that matched well with the reported pattern [12]. With an increase of titanium content (decrease of Si/Ti ratio), the XRD patterns, especially higher order Bragg reflections, become poorly resolved and the XRD peaks are broaden, which could be attributed to decrease in the structural integrity. The intensity of (1 0 0) peak decreased with an increase of titanium content and this may be due to the formation of non-framework metal oxide species inside the mesopores [13].

For TiO_2 loaded Ti-SBA-15 samples, the second part of XRD analysis was carried out in the range of 10–70° in order to assess the crystallinity of TiO_2. As shown in Fig. 3(b), the TiO_2 particles loaded on Ti-SBA-15 material seem to have mainly anatase structure. The intensity of (1 0 1) peak increases with an increase of titanium dioxide loading ratio. This indicates that the crystallite size of titanium dioxide increases due to the agglomeration of titania particles with an increase of titanium dioxide loading ratio.

Fig. 4 shows the IR spectra of Ti-SBA-15 and TiO_2/Ti-SBA-15 materials. For Ti-SBA-15 samples, the IR absorption at about 960 cm^{-1} commonly accepted the characteristic vibration of Ti–O–Si bond. In the present work, the band at about 960 cm^{-1} is rather weak in pure siliceous SBA-15 and this band increases in its intensity as titanium content is increased. This result indicates that systematic increase in intensity of IR absorption with increasing titanium amount is generally taken as a proof of Ti incorporating into the framework of zeolite [14]. Therefore, it is thought that the incorporation of titanium into framework increases the symmetry of local structure of SBA-15, which causes to increase the intensity of the band at about 960 cm^{-1}. The wave number of ~800 cm^{-1} in Fig. 4 indicate the band for Si–O–Si bond.

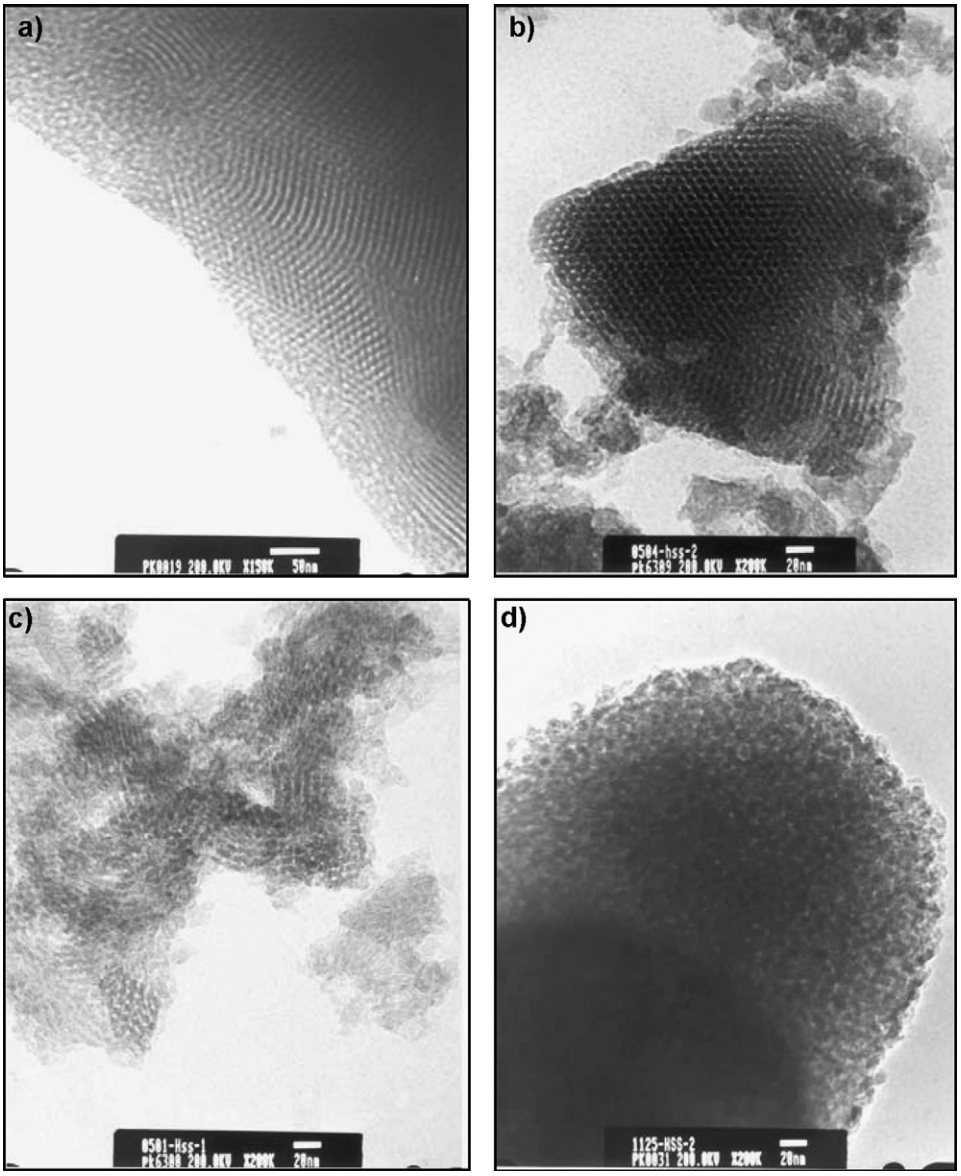

Fig. 6. TEM images of SBA-15 (a), Ti-SBA-15 (Si/Ti = 50) (b), Ti-SBA-15 (Si/Ti = 10) (c), and TiO_2/Ti-SBA-15 (d) materials.

For the TiO_2/Ti-SBA-15 samples, similar results are obtained on the characteristic vibration of Ti–O–Si bond at ~960 cm^{-1}.

UV–vis spectroscopy has been used widely for the characterization of the nature and coordination of Ti^{4+} ions in titanium-substituted molecular sieves [4,15]. According to Jorgensen's and Lippard classification [16] and more recently that of Boccuti et al. [17], the existence titanium(IV) isolated in the framework is characterized by a band at about 210–230 nm for a tetrahedral environment and 240–250 nm for an octahedral environment. The formation of titanium dioxide clusters in the anatase form leads to a displacement of the band towards higher wavelengths. Thus, the absorption threshold for anatase is at about 330 nm. The UV–vis diffuse reflectance spectra of the of Ti-SBA-15 and TiO_2/Ti-SBA-15 samples prepared in our study are shown in Fig. 5. Without titanium ion, SBA-15 exhibits no absorption at 220 nm. However, the Ti-SBA-15 samples having Si/Ti ratio higher than 20 shows the band at 220 nm, indicating framework incorporation of titanium into SBA-15. On the other hand, the intensity of the band at about 330 nm increases monotonically with an increase of titanium content. This can be attributed the presence of foreign ions with relatively high concentration in the gel during synthesis, which can hinder the structure-directing action of the template by changing the ionic strength of the medium [18], probably resulting in low structural integrity and formation of titanium oxide clusters.

For the TiO_2/Ti-SBA-15 samples, similar results are obtained on the UV–vis diffuse reflectance spectra. However, TiO_2 loaded Ti-SBA-15 samples shows no absorption at 220 nm. The band at 330 nm increases monotonically with an increase of titanium dioxide loading amount and the spectrum of 50 wt.% TiO_2-loaded samples is almost identical to that of pure TiO_2.

TEM pictures of SBA-15, Ti-SBA-15 and TiO_2/Ti-SBA-15 samples are shown in Fig. 6. The highly ordered structure of pure SBA-15 is shown as described in literature [10,19]. Moreover, the regular silica morphology is maintained in the case of Ti-SBA-15(50:1) but the Ti-SBA-15 sample having Si/Ti ratio = 10 makes partially to destroy the hexagonal highly ordered structure.

As shown in Fig. 6(d), for the 50 wt.% TiO_2/Ti-SBA-15 samples, the highly ordered mesopore structure is disappeared by the clogging of mesopore channels by the titanium dioxides particles

Fig. 7 shows photocatalytic decomposition of orange II over Ti-SBA-15(a) and TiO_2/Ti-SBA-15(b) catalysts under UV illumination.

It is well known that photocatalytic oxidation of organic pollutants follows Langmuir–Hinshelwood kinetics [2,20], with the rate being proportional to the coverage θ:

$$r = -\frac{dc}{dt} = k\theta = k\frac{KC}{1+KC} \quad (1)$$

where k is the true rate constant which is dependent upon various parameters such as mass of catalyst, the flux of efficient, the coverage in oxygen, etc., K the adsorption coefficient of the reactant, and C the reactant concentration. When C is very small, the product KC is negligible with respect to unity so that Eq. (1) describes a first-order kinetics. Setting the Eq. (1) at the initial conditions of the photocatalytical procedure, $t = 0$, the concentration transforms to $C = C_0$, which gives Eq. (2).

$$-\ln\left(\frac{C}{C_o}\right) = k_{app}t \quad (2)$$

where k_{app} is the apparent first-order reaction constant.

The photocatalytic activity on the decomposition of orange II is shown in Table 1. When blank test in the absence of photocatalyst was carried out, orange II was decomposed to about 10% after 3 h reaction by photolysis reaction. The photocatalytic activity increases with an increase of Ti content (decrease of Si/Ti ratio). This result indicates that the titanium incorporated into SBA-15 framework plays an important role on the decomposition of orange II and acts as photocatalytic active sites. It can be also thought that the anatse TiO_2 particles are formed in the case of Ti-substituted SBA-15 materials owing to the existence of oxygen in the cage of mesoporous materials [7,12]. Therefore, the improvement in the photocatalytic activity should be attributed to the formation of anatase TiO_2 particles on the external surface with an increase of Ti incorporation amount.

The photocatalytic activity of the TiO_2/Ti-SBA-15 catalysts is shown higher values than Ti-SBA-15 catalyst. It is thought that the photocatalytic reaction can be happened on both sites of

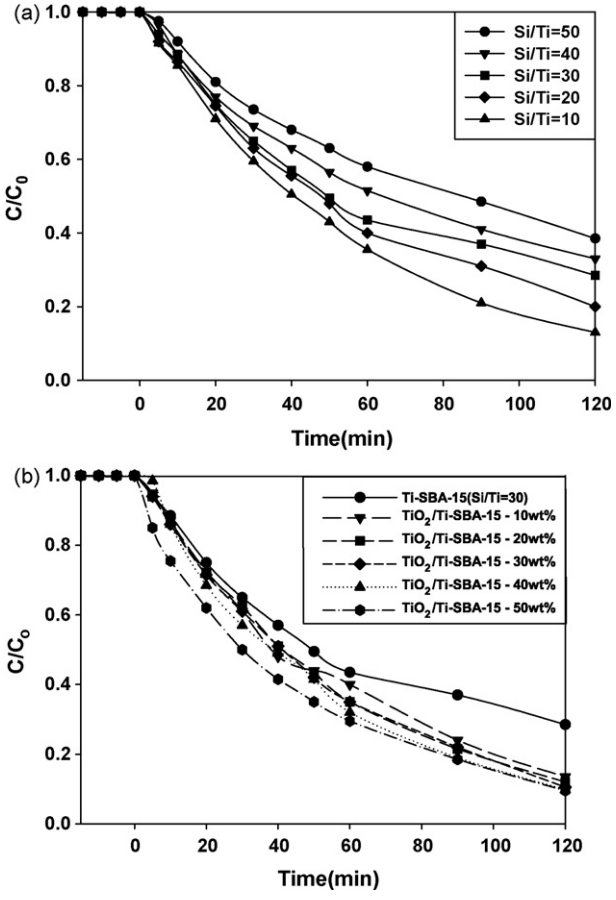

Fig. 7. Photocatalytic decomposition of orange II over various Ti-SBA-15 (a) and TiO_2/Ti-SBA-15 materials (b).

TiO_2 particles consisted of bulk TiO_2 and TiO_2 particles formed by incorporation of titanium. For the TiO_2/Ti-SBA-15 catalysts, the photocatalytic activity increases with an increase of TiO_2 loading ratio. It is thought that the increase of crystallinity of anatase structure with increasing TiO_2 loading content gives a rise to increment on the photocatalytic activity.

4. Conclusions

Titanium substituted SBA-15 mesoporous material has been successfully prepared by conventional hydrothermal method and they were also used as support on TiO_2 loaded Ti-SBA-15 photocatalysts. The synthesized materials were characterized by XRD, DRS, FT-IR, BET and TEM. We also examined the activity of these materials as photocatalysts for the decomposition of orange II. It is clear that the incorporation of titanium into framework of SBA-15 makes the pore diameter and pore volume to decrease, due to the fact that the diameter of a titanium atom is larger than that of a silicon atom, but slightly decreases the surface area compared to SBA-15. In addition, titania loaded on the silica matrix decreases the surface area of the support as expected for TiO_2 incorporation. This result can be confirmed by the TEM micrograph of 50 wt% loaded TiO_2 on Ti-SBA-15 which the highly ordered mesopore structure is disappeared by the clogging of mesopore channels by the titanium dioxides particles. From the XRD results, calcined siliceous SBA-15 and Ti-SBA-15 samples with varying titanium loading displayed well-resolved pattern with a sharp peak at about 1.0°. For Ti-SBA-15 and TiO_2 loaded Ti-SBA-15 photocatalysts, the IR absorption at $\sim$960 cm^{-1} commonly accepted the characteristic vibration of Ti–O–Si bond. From the TEM images, the regular silica morphology is maintained in the case of Ti-SBA-15 (Si/Ti = 50) but the Ti-SBA-15 sample having Si/Ti ratio = 10 makes partially to destroy the hexagonal highly ordered structure and the mesopore structure is disappeared by the clogging of mesopore channels by the titanium dioxides particles for the 50 wt.% TiO_2/Ti-SBA-15 samples. The photocatalytic activity increases with an increase of Ti content (decrease of Si/Ti ratio) and with an increase of TiO_2 loading content.

Acknowledgements

This work was supported by the Korea Research Foundation Grant funded by the Korea Government (MOEHRD)(KRF-2005-041-D00206) and was supported by the Program for the Training of Graduate Students in Regional Innovation which was conducted by the Ministry of Commerce, Industry and Energy of the Korean Government.

References

[1] Y.B. Ryu, S.S. Park, G.D. Lee, S.S. Hong, J. Ind. Eng. Chem. 12 (2006) 289.
[2] S.S. Hong, M.S. Lee, J.H. Kim, B.H. Ahn, K.T. Lim, G.D. Lee, J. Ind. Eng. Chem. 8 (2002) 150.
[3] R.L. Pozzo, M.A. Baltanas, A.E. Cassano, Catal. Today 39 (1997) 219.
[4] B. Notari, Adv. Catal. 41 (1996) 253.
[5] Y.J. Do, J.H. Kim, J.H. Park, S.S. Park, S.S. Hong, C.S. Suh, G.D. Lee, Catal. Today 101 (2005) 299.
[6] D. Zhao, Q. Huo, J. Feng, B.F. Chmelka, G.D. Stucky, J. Am. Chem. Soc. 120 (1998) 6024.
[7] B.L. Newalkar, J. Olanrewaju, S. Komarneni, Chem. Mater. 13 (2001) 552.
[8] Y. Chen, Y.L. Huang, J.H. Xiu, X.W. Han, X.H. Bao, Appl. Catal., A 273 (2004) 185.
[9] R. van Grieken, J. Aguado, M.J. Lopez-Munoz, J. Marugan, J. Photochem. Photobiol. A 148 (2002) 305.
[10] M.J. Lopez-Munoz, R. van Grieken, J. Aguado, J. Marugan, Catal. Today 101 (2005) 307.
[11] S.J. Gregg, K.S.W. Sing, Adsorption, Surface Area and Porosity, Academic Press, London, 1982.
[12] G. Li, X.S. Zhao, Ind. Eng. Chem. Res. 45 (2006) 3569.
[13] M. Karthik, A.K. Tripathi, N.M. Gupta, A. Vinu, M. Hartmann, M. Palanichany, V. Murugesan, Appl. Catal., A 268 (2004) 139.
[14] M.D. Alba, Z. Luan, J. Klinowski, J. Phys. Chem. 100 (1996) 2178.
[15] A. Tuel, Zeolite 15 (1995) 228.
[16] C.K. Jorgensen, S.J. Lippard (Eds.), Prog. Inorg. Chem., Wiley, New York, 1970, p. 12.
[17] M. Boccuti, K.M. Rao, A. Zecchina, G. Leofanti, G. Petrini, in: C. Morterra, A. Zecchina, G. Costa (Eds.), Structure and Reactivity of Surfaces, Elsevier, Amsterdam, 1989, p. 133.
[18] E.P. reddy, L. Davydov, P.G. Smirniotis, J. Phys. Chem., B 106 (2002) 3394.
[19] D. Zhao, J. Feng, Q. Huo, N. Melosh, G.H. Fredrickson, B.F. Chmelka, G.D. Stucky, Science 279 (1998) 6024.
[20] C.S. Turchi, D.F. Ollis, J. Catal. 122 (1995) 178.